



# Interaction of NO<sub>2</sub> with TiO<sub>2</sub> surface under UV irradiation: measurements of the uptake coefficient

A. El Zein, Y Bedjanian

## ► To cite this version:

A. El Zein, Y Bedjanian. Interaction of NO<sub>2</sub> with TiO<sub>2</sub> surface under UV irradiation: measurements of the uptake coefficient. *Atmospheric Chemistry and Physics*, 2012, 12, pp.1013-1020. 10.5194/acp-12-1013-2012 . insu-01323370

**HAL Id: insu-01323370**

**<https://insu.hal.science/insu-01323370>**

Submitted on 30 May 2016

**HAL** is a multi-disciplinary open access archive for the deposit and dissemination of scientific research documents, whether they are published or not. The documents may come from teaching and research institutions in France or abroad, or from public or private research centers.

L'archive ouverte pluridisciplinaire **HAL**, est destinée au dépôt et à la diffusion de documents scientifiques de niveau recherche, publiés ou non, émanant des établissements d'enseignement et de recherche français ou étrangers, des laboratoires publics ou privés.



Distributed under a Creative Commons Attribution - NonCommercial - NoDerivatives 4.0 International License



# Interaction of NO<sub>2</sub> with TiO<sub>2</sub> surface under UV irradiation: measurements of the uptake coefficient

A. El Zein and Y. Bedjanian

Institut de Combustion, Aérodynamique, Réactivité et Environnement (ICARE), CNRS-INSU, OSUC (UMS3116), 45071 Orléans Cedex 2, France

Correspondence to: Y. Bedjanian (yuri.bedjanian@cnrs-orleans.fr)

Received: 27 September 2011 – Published in Atmos. Chem. Phys. Discuss.: 12 October 2011

Revised: 17 January 2012 – Accepted: 17 January 2012 – Published: 20 January 2012

**Abstract.** The interaction of NO<sub>2</sub> with TiO<sub>2</sub> solid films was studied under UV irradiation using a low pressure flow reactor (1–10 Torr) combined with a modulated molecular beam mass spectrometer for monitoring of the gaseous species involved. The NO<sub>2</sub> to TiO<sub>2</sub> reactive uptake coefficient was measured from the kinetics of NO<sub>2</sub> loss on TiO<sub>2</sub> coated Pyrex rods as a function of NO<sub>2</sub> concentration, irradiance intensity ( $J_{\text{NO}_2} = 0.002\text{--}0.012\text{ s}^{-1}$ ), relative humidity (RH = 0.06–69 %), temperature ( $T = 275\text{--}320\text{ K}$ ) and partial pressure of oxygen (0.001–3 Torr). TiO<sub>2</sub> surface deactivation upon exposure to NO<sub>2</sub> was observed. The initial uptake coefficient of NO<sub>2</sub> on illuminated TiO<sub>2</sub> surface (with 90 ppb of NO<sub>2</sub> and  $J_{\text{NO}_2} \cong 0.006\text{ s}^{-1}$ ) was found to be  $\gamma_0 = (1.2 \pm 0.4) \times 10^{-4}$  (calculated using BET surface area) under dry conditions at  $T = 300\text{ K}$ . The steady state uptake,  $\gamma$ , was several tens of times lower than the initial one, independent of relative humidity, and was found to decrease in the presence of molecular oxygen. In addition, it was shown that  $\gamma$  is not linearly dependent on the photon flux and seems to level off under atmospheric conditions. Finally, the following expression for  $\gamma$  was derived,  $\gamma = 2.3 \times 10^{-3} \exp(-1910/T)/(1 + P^{0.36})$  (where  $P$  is O<sub>2</sub> pressure in Torr), and recommended for atmospheric applications (for any RH, near 90 ppb of NO<sub>2</sub> and  $J_{\text{NO}_2} = 0.006\text{ s}^{-1}$ ).

geneous reactions, to HNO<sub>3</sub>, which remains on the TiO<sub>2</sub> surface (Ibusuki and Takeuchi, 1994; Dalton et al., 2002; Devahasdin et al., 2003; Negishi et al., 1998; Ohko et al., 2008). Due to these photocatalytic properties TiO<sub>2</sub> is widely used in a variety of so-called de-polluting building materials aimed to remove the nitrogen oxides from the atmosphere.

However, the antipolluting nature of the TiO<sub>2</sub>-containing materials was recently questioned (Langridge et al., 2009; Monge et al., 2010; Ndour et al., 2009a). Ndour et al. (2009a) have shown that nitrate ions adsorbed onto mixed TiO<sub>2</sub>/SiO<sub>2</sub> and pure TiO<sub>2</sub> can be converted into gaseous NO and NO<sub>2</sub> under UV irradiation. Moreover, it was shown that the interaction of NO<sub>2</sub> with TiO<sub>2</sub> (Monge et al., 2010) and commercial self-cleaning TiO<sub>2</sub>-containing window glass (Langridge et al., 2009) results in the formation of nitrous acid (HONO) in the gas phase, that may have a negative environmental impact (Monge et al., 2010). In contrast, Laufs et al. (2010) working with TiO<sub>2</sub> doped commercial paints observed an efficient decomposition of HONO on the photolytic samples and concluded that the paint surfaces do not represent a source of HONO. So the question seems to remain open, pending further studies.

Titanium dioxide, although being a minor component of mineral dust particles (Karagulian et al., 2006), was shown recently to be responsible for the photochemical reactivity of atmospheric mineral aerosols (Ndour et al., 2008). Thus the information on the photoinitiated uptake of atmospheric trace gases to TiO<sub>2</sub> surface is of great importance for the modelling of the day time chemistry of the atmosphere. Only a few studies are known, in which the uptake coefficient of NO<sub>2</sub> to irradiated pure TiO<sub>2</sub> or TiO<sub>2</sub>-doped surfaces was measured (Gustafsson et al., 2006; Monge et al., 2010; Ndour et al.,

## 1 Introduction

Titanium dioxide (TiO<sub>2</sub>) is a very efficient photocatalyst leading to the degradation of organic species under UV irradiation (e.g. Henderson, 2011). In addition, TiO<sub>2</sub> is known to transform nitrogen oxides (NO/NO<sub>2</sub>), via catalytic hetero-

2008, 2009b). The information available for the uptake coefficient of NO<sub>2</sub> to the illuminated TiO<sub>2</sub> surface remains limited and will be discussed below in association with the data from the present study.

On the basis of the above information, it is clear that complementary studies are needed in order to better determine both the rate and products of the NO<sub>2</sub> interaction with illuminated pure TiO<sub>2</sub>, real mineral aerosols, as well as with different de-polluting building materials containing TiO<sub>2</sub>. This paper reports results of measurements of the uptake coefficient of NO<sub>2</sub> to the TiO<sub>2</sub> surface as a function of different parameters such as NO<sub>2</sub> concentration, irradiance intensity, relative humidity, temperature and partial pressure of oxygen. A detailed study of the reaction products is the subject of our ongoing research.

## 2 Experimental

### 2.1 Preparation of TiO<sub>2</sub> films

Solid TiO<sub>2</sub> films were deposited on the outer surface of a Pyrex tube (0.9 cm i.d.) using a TiO<sub>2</sub> (Sigma Aldrich, Aeroxide P25, (50±15) m<sup>2</sup>g<sup>-1</sup> surface area, ~20 nm particle diameter) suspension in ethanol. Prior to film deposition, the Pyrex tube was treated with hydrofluoric acid and washed with distilled water and ethanol. Then the tube was immersed into the suspension, withdrawn and dried with a fan heater. As a result rather homogeneous (to the eye) films of TiO<sub>2</sub> were formed at the Pyrex surface. In order to eliminate possible residual traces of ethanol, prior to uptake experiments, the freshly prepared TiO<sub>2</sub> samples were heated at (100–150) °C during (20–30) min under pumping. In order to measure the mass of the sample on the Pyrex tube the deposited TiO<sub>2</sub> film was mechanically removed at the end of the kinetic experiments.

### 2.2 Flow reactor

Interaction of NO<sub>2</sub> with solid TiO<sub>2</sub> films was studied at 1–10 Torr total pressure (He being used as the carrier gas with 0.07–0.35 SLM flow rate) using the flow tube technique with mass spectrometric detection of the gaseous species involved. A modulated molecular beam mass spectrometer (BALZERS QMG 420) was used. The molecular beam, resulting from a differential pumping system, was modulated in the first vacuum chamber, allowing for a synchronous detection via a lock-in amplifier. In the second vacuum chamber containing the quadrupole mass spectrometer, the electron impact ion source (operating at 25–30 eV energy) was surrounded by a copper device cooled by liquid nitrogen, which allowed to significantly reduce the background spectrum. This chamber was pumped by means of a turbomolecular pump. The ions were detected via an electron multiplier. All the species were detected at their parent peaks. A typical detection limit for NO<sub>2</sub> was nearly  $2 \times 10^{10}$  molecules cm<sup>-3</sup>.

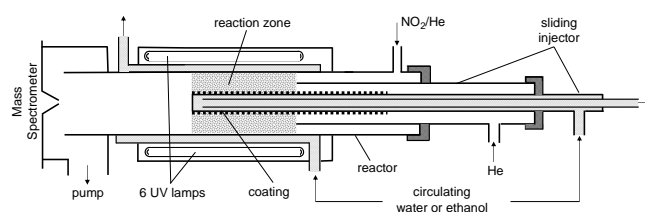
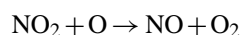


Fig. 1. Diagram of the flow photoreactor used.

The absolute concentration of NO<sub>2</sub> in the reactor was calculated from its flow rate obtained from the measurements of the pressure drop of a NO<sub>2</sub>/He mixture in a calibrated volume flask. H<sub>2</sub>O was introduced into the reactor by flowing He through a bubbler containing thermostated water. The H<sub>2</sub>O flow rate was calculated from the H<sub>2</sub>O vapor pressure and total (H<sub>2</sub>O + He) pressure and the measured flow rate of He through the bubbler.

The main reactor (Fig. 1) consisted of a Pyrex tube (40 cm length and 2.4 cm i.d.) with a jacket for the thermostated liquid circulation. Experiments were carried out using a coaxial configuration of the flow reactor with movable triple central injector: the Pyrex tube with deposited sample was introduced into the main reactor along its axis. This tube could be moved relative to the outer tube of the injector. This allowed the variation of the sample length exposed to NO<sub>2</sub>. The third (inner) tube of the movable injector was used for circulation of the thermostated liquid inside the tube covered with TiO<sub>2</sub> sample. This allowed maintaining the same temperature in the main reactor and on the sample surface in the measurements of the temperature dependence. In addition, the sample could be heated up to a few hundreds °C by means of a coaxial cylindrical heater which could be introduced inside the tube with the sample.

The reactor was surrounded by 6 lamps (Sylvania BL350, 8 W, 315–400 nm with peak at 352 nm). The actinic flux inside the reactor was not measured in the present study, however, in order to characterize the irradiance intensity in the reactor we have directly measured the NO<sub>2</sub> photolysis frequency as a function of the number of lamps switched on. In these experiments NO<sub>2</sub> was introduced into the photoreactor through the central tube of the movable injector (shadowed to prevent NO<sub>2</sub> photolysis inside it) and the concentration of NO<sub>2</sub> was monitored by the mass spectrometer as a function of the NO<sub>2</sub> residence time (up to 13 s) in the irradiated part of the reactor. Experiments were carried out with rather high NO<sub>2</sub> concentrations ( $\sim 10^{14}$  molecule cm<sup>-3</sup>). Under such experimental conditions, the loss of NO<sub>2</sub> is due to two processes: NO<sub>2</sub> photolysis  $\text{NO}_2 + h\nu \rightarrow \text{NO} + \text{O}$  and a secondary reaction with oxygen atoms



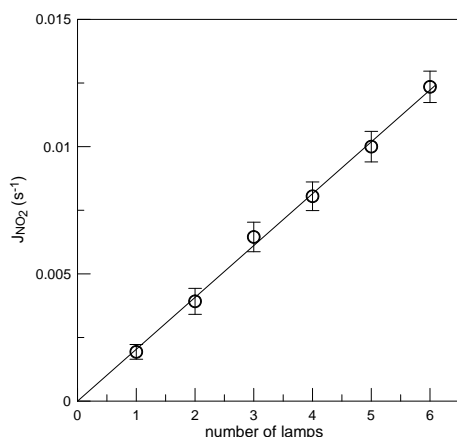


**Fig. 2.** Photolysis frequency of  $\text{NO}_2$  ( $J_{\text{NO}_2}$ ) as a function of the number of UV lamps switched on.

This latter being much faster than  $\text{NO}_2$  photolysis, the rate of  $\text{NO}_2$  loss is:

$$d[\text{NO}_2]/dt = -2 J_{\text{NO}_2}[\text{NO}_2]$$

The values of  $J_{\text{NO}_2}$  determined from the exponential decays of  $\text{NO}_2$  for different numbers of lamps switched on are shown in Fig. 2. One can note that the resulting values of  $J_{\text{NO}_2}$  in our system (from 0.002 to  $0.012 \text{ s}^{-1}$ ) are close to the corresponding values in the atmosphere.

### 2.3 Data analysis

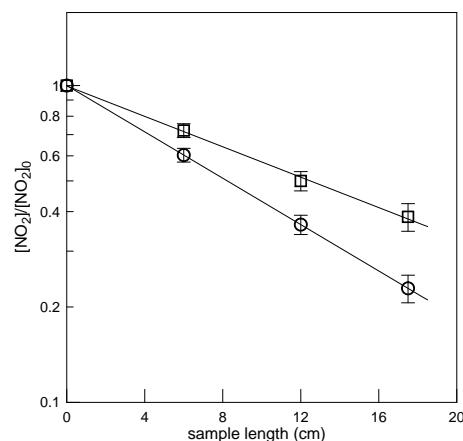
The purpose of this study was to measure the uptake coefficient of  $\text{NO}_2$  ( $\gamma$ ) determined as the probability of reactive  $\text{NO}_2$  loss per collision with the  $\text{TiO}_2$  surface:

$$\gamma = \frac{4k' V}{\omega S}$$

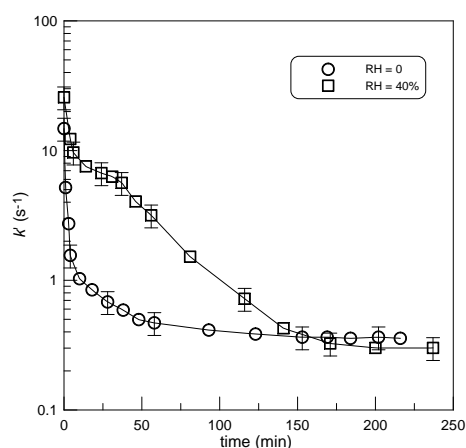
where  $k'$  ( $\text{s}^{-1}$ ) is the first-order rate constant of  $\text{NO}_2$  loss,  $\omega$  the average molecular speed ( $355.9\text{--}383.9 \text{ m s}^{-1}$  for  $T = 275\text{--}320 \text{ K}$ ),  $V$  the volume of the reaction zone, and  $S$  the surface area of the  $\text{TiO}_2$  sample. To calculate the uptake coefficient, two parameters should be determined experimentally: the rate constant  $k'$  and the  $\text{TiO}_2$  film surface area accessible to  $\text{NO}_2$ .

Figure 3 displays examples of  $\text{NO}_2$  loss kinetics in the heterogeneous reaction with the  $\text{TiO}_2$  surface. These data were obtained by varying the length of the  $\text{TiO}_2$  film in contact with  $\text{NO}_2$ , which is equivalent to varying the reaction time. The  $\text{NO}_2$  decays were found to be exponential and were treated with the first-order kinetics formalism, the rate constant being determined as:

$$k' = -\frac{d\ln([\text{NO}_2])}{dt}$$



**Fig. 3.** Examples of kinetics of  $\text{NO}_2$  consumption on  $\text{TiO}_2$  surface:  $T = 300 \text{ K}$ , sample mass =  $0.3 \text{ mg cm}^{-1}$ ,  $J_{\text{NO}_2} \approx 0.006 \text{ s}^{-1}$ . Circles: initial uptake,  $P = 1 \text{ Torr}$ ,  $[\text{NO}_2] = 3.3 \times 10^{12} \text{ molecule cm}^{-3}$ , flow velocity =  $420 \text{ cm s}^{-1}$ ; squares:  $P = 9 \text{ Torr}$ , exposure time =  $150 \text{ min}$ ,  $[\text{NO}_2] = 1.5 \times 10^{12} \text{ molecule cm}^{-3}$ , flow velocity =  $42 \text{ cm s}^{-1}$ .



**Fig. 4.** Dependence of the first order rate constant of  $\text{NO}_2$  loss on  $\text{TiO}_2$  surface upon exposure time:  $T = 280 \text{ K}$ ,  $P = 1\text{--}9 \text{ Torr}$ ,  $J_{\text{NO}_2} \approx 0.006 \text{ s}^{-1}$ , sample mass  $\approx 0.4 \text{ mg cm}^{-1}$ ,  $[\text{NO}_2] \approx 10^{13} \text{ molecule cm}^{-3}$ .

where  $t$  is the reaction time defined by the ratio sample length/flow velocity. The values of the first-order rate constants,  $k'$ , determined from the decays of  $\text{NO}_2$  were corrected for the diffusion limitation in the  $\text{NO}_2$  radial transport from the volume to the reactive surface of the reactor (Bedjanian et al., 2005 and refs therein). Corrections applied to  $k'$  did not exceed 10%.

The data presented in Fig. 3 show a decrease of the  $\text{NO}_2$  loss rate with exposure time indicating  $\text{TiO}_2$  sample deactivation during the heterogeneous reaction: the value of  $k'$  for initial uptake is much higher than that observed after 150 min of exposure to  $\text{NO}_2$  (note, that the flow velocities corresponding

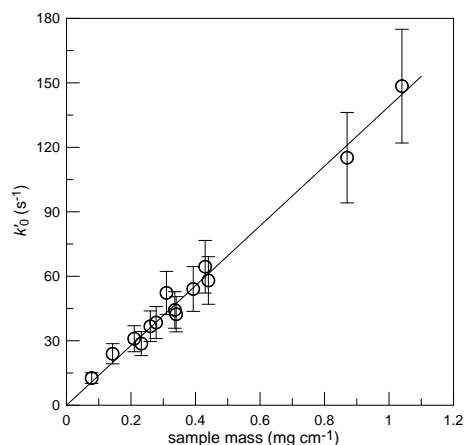


**Fig. 5.** Dependence of the initial rate of  $\text{NO}_2$  loss on the mass of  $\text{TiO}_2$  sample (per 1 cm length of the support tube):  $P = 1$  Torr,  $T = 300$  K,  $J_{\text{NO}_2} \cong 0.006 \text{ s}^{-1}$ ,  $[\text{NO}_2] \sim 10^{12} \text{ molecule cm}^{-3}$ .

to the two curves in Fig. 3 differ by a factor of 10). Dependence of  $k'$  upon the exposure time of the  $\text{TiO}_2$  film to  $\text{NO}_2$  is shown in Fig. 4. One can note that the rate of  $\text{NO}_2$  loss is decreasing with time approaching a steady state value after approximately 2 h of exposure. This value, under the conditions of these experiments, is by a factor near 50 lower than the rate of initial  $\text{NO}_2$  uptake,  $k'_0$ , corresponding to the first seconds of the  $\text{TiO}_2$  sample exposure to  $\text{NO}_2$ . The data presented in Fig. 4 show that the steady state values of  $k'$  are very similar for dry conditions and 40% RH, although the  $\text{TiO}_2$  sample deactivation is faster under dry conditions.

Specific experiments have been carried out in order to determine the  $\text{TiO}_2$  surface area involved in interaction with  $\text{NO}_2$  under experimental conditions used. For that, the  $\text{NO}_2$  loss rate  $k'$  was measured as a function of the thickness of  $\text{TiO}_2$  coating. The results observed for the initial (corresponding to the first 10–30 s of exposure) uptake of  $\text{NO}_2$  on  $\text{TiO}_2$  are shown in Fig. 5 as a dependence of the rate constant of  $\text{NO}_2$  loss on the mass of  $\text{TiO}_2$  deposited per unity length of the support tube (equivalent to the thickness of the coating which was assumed to be homogeneous and evenly dense). The observed linear dependence of the reaction rate on the thickness of the  $\text{TiO}_2$  film indicates that the entire surface area of the  $\text{TiO}_2$  samples (at least, for samples with masses up to  $1 \text{ mg cm}^{-1}$ ) is involved in the interaction with  $\text{NO}_2$  and, consequently, the BET surface area should be used for calculations of the uptake coefficient. The data presented in Fig. 5 provide the following value for the initial uptake coefficient of  $\text{NO}_2$  on the illuminated  $\text{TiO}_2$  surface ( $J_{\text{NO}_2} \cong 0.006 \text{ s}^{-1}$ ) under dry conditions at  $T = 300$  K:

$$\gamma_0 = (1.2 \pm 0.4) \times 10^{-4}$$

where the uncertainty includes the statistical one and those on the BET surface area and on the measurements of  $k'_0$ . It should be noted that the value obtained for  $\gamma_0$ , being

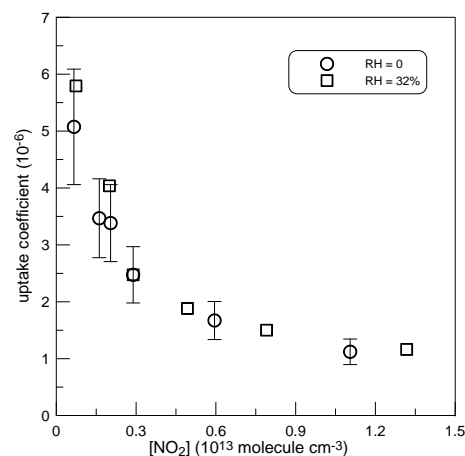


**Fig. 6.** Uptake coefficient as function of the initial concentration of  $\text{NO}_2$ :  $T = 280$  K,  $P = 9$  Torr,  $J_{\text{NO}_2} \cong 0.006 \text{ s}^{-1}$ , sample mass =  $0.32 \text{ mg cm}^{-1}$ . Error bars represent estimated 20 % uncertainty on the measurements of  $\gamma$ .

calculated with the BET surface area ( $50 \text{ m}^2 \text{ g}^{-1}$ ), should be considered as a lower limit. On the other hand, the upper limit of  $\gamma_0$  can also be estimated. Thus, applying the geometric (projected) surface area to the data observed with the smallest mass of  $\text{TiO}_2$  used in these experiments (Fig. 5,  $m = 0.08 \text{ mg cm}^{-1}$ ,  $k'_0 = 12.7 \text{ s}^{-1}$ ) one gets the value of  $1.9 \times 10^{-3}$  for the uptake coefficient which is an upper limit of  $\gamma_0$ .

Similar experiments carried out under dark conditions allowed to determine the initial uptake coefficient of  $\text{NO}_2$  on  $\text{TiO}_2$  in the absence of irradiation (calculated with BET surface area):

$$\gamma_0(\text{dark}) = (6.0 \pm 2.0) \times 10^{-6}$$

under dry conditions at  $T = 300$  K.

### 3 Results

The present study was focused on the determination of the steady state value of  $\gamma$  as a function of different parameters; even though the initial uptake was measured under certain experimental conditions (see above). The experimental data presented below for the uptake coefficient,  $\gamma$ , correspond to its steady state value. Experiments were carried out with  $\text{TiO}_2$  masses near  $0.3 \text{ mg cm}^{-1}$  at total pressure of 9–10 Torr of Helium in the reactor and mostly at  $T = 280$  K. This relatively low temperature was chosen as the standard temperature of this study in order to be able to ensure a reasonable level of relative humidity at the rather low total pressure in the reactor.

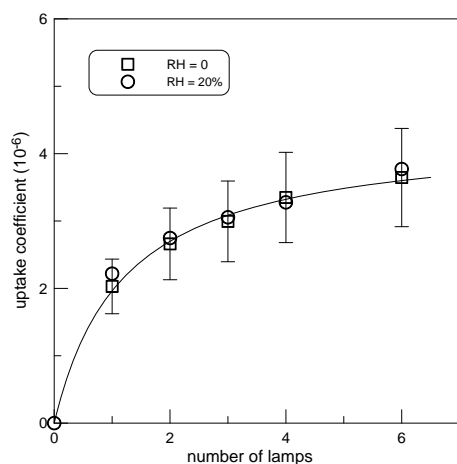


**Fig. 7.** Uptake coefficient as a function of the irradiation intensity (number of lamps switched on):  $T = 280$  K,  $P = 9$  Torr, sample mass =  $0.47 \text{ mg cm}^{-1}$ ,  $[\text{NO}_2] \approx 2 \times 10^{12} \text{ molecule cm}^{-3}$ . The line is drawn to guide the eye.

### 3.1 Dependence on $\text{NO}_2$ concentration

The dependence of  $\gamma$  on the gas phase concentration of  $\text{NO}_2$  measured under dry conditions and  $\text{RH} = 32\%$  with  $[\text{NO}_2]_0$  varied in the range  $(0.06\text{--}1.32) \times 10^{13} \text{ molecule cm}^{-3}$  is shown in Fig. 6. One can note that the uptake coefficient decreases upon increase of the initial  $\text{NO}_2$  concentration. The negative dependence on  $[\text{NO}_2]$  may be due to the surface saturation by the adsorbed precursor and/or depletion of photo-produced intermediates. With the purpose of comparison, the measurements of the uptake coefficient under different experimental conditions presented below were carried out with the initial concentration of  $\text{NO}_2$  fixed at nearly  $2 \times 10^{12} \text{ molecule cm}^{-3}$ . This value is the result of a compromise between the need to work at lower concentrations and the  $\text{NO}_2$  detection sensitivity.

### 3.2 Dependence on irradiation intensity

Dependence of the uptake coefficient on the illumination intensity was studied by switching on the different number of lamps in the reactor, from 1 to 6. As shown above, this corresponds to the variation of the  $\text{NO}_2$  photolysis frequency from 0.002 to  $0.012 \text{ s}^{-1}$ . The results obtained under dry conditions and at  $\text{RH} = 20\%$  are shown in Fig. 7. One can note that less than two-fold increase of  $\gamma$  is observed whereas the irradiation intensity is changed by a factor of 6. This observation seems to be of great importance as it shows that the  $\gamma$ -values measured at low irradiation intensities could not be extrapolated in a linear way to those relevant to the atmosphere. The three series of experiments presented below were carried out using 3 lamps switched on ( $J_{\text{NO}_2} \approx 0.006 \text{ s}^{-1}$ ).

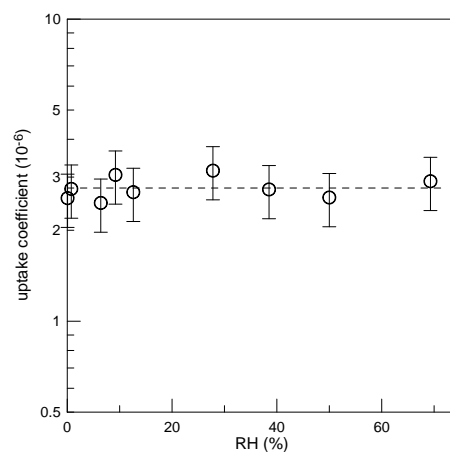


**Fig. 8.** Uptake coefficient as a function of relative humidity:  $T = 280$  K,  $P = 9$  Torr,  $J_{\text{NO}_2} \approx 0.006 \text{ s}^{-1}$ , sample mass =  $0.38 \text{ mg cm}^{-1}$ ,  $[\text{NO}_2] \approx 2 \times 10^{12} \text{ molecule cm}^{-3}$ ,  $\text{RH} = (0.06\text{--}69)\%$ .

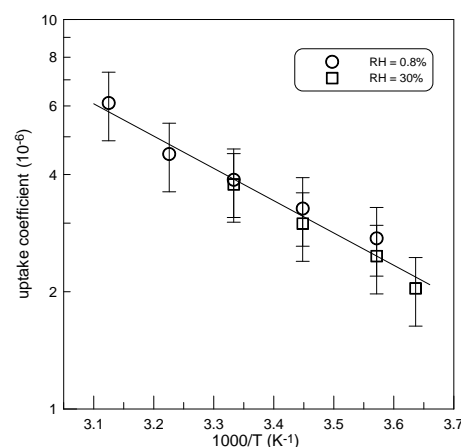


**Fig. 9.** Temperature dependence of the uptake coefficient measured at  $T = 275\text{--}320$  K under 0.8 and 30% relative humidity:  $P = 9$  Torr,  $J_{\text{NO}_2} \approx 0.006 \text{ s}^{-1}$ , sample mass =  $0.34 \text{ mg cm}^{-1}$ ,  $[\text{NO}_2] \approx 2 \times 10^{12} \text{ molecule cm}^{-3}$ .

### 3.3 Dependence on relative humidity

The data presented in Figs. 4, 6 and 7 observed under different relative humidity in the reactor show that the steady state uptake coefficient is not sensitive to this parameter. Figure 8 displays the results of the measurements of  $\gamma$  in the extended range of RH, from 0.06 to 69%. The presented data clearly show that the uptake coefficient is independent of RH in this range. The dashed line in Fig. 8 corresponds to the mean value of  $\gamma = 2.8 \times 10^{-6}$ .

### 3.4 Dependence on temperature

The temperature dependence of the uptake coefficient measured in the temperature range (275–320) K is shown in

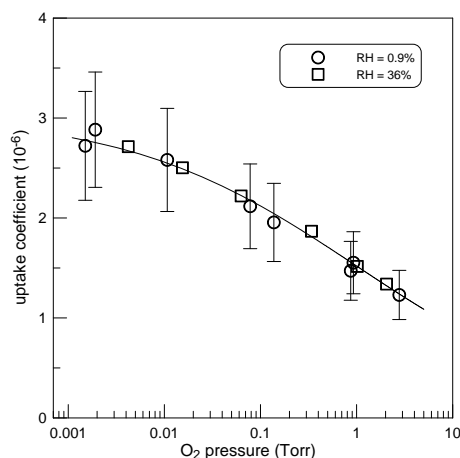


**Fig. 10.** Uptake coefficient as a function of partial pressure of oxygen:  $T = 280$  K,  $P = 9$  Torr,  $J_{\text{NO}_2} \approx 0.006 \text{ s}^{-1}$ , sample mass  $= 0.38 \text{ mg cm}^{-2}$ ,  $[\text{NO}_2] \approx 2 \times 10^{12} \text{ molecule cm}^{-3}$ .

Fig. 9. The uptake coefficient is found to increase with increasing temperature. The data observed with two different RH at  $T = 280$ , 290 and 300 K are similar in the range of experimental uncertainty indicating insignificant RH dependence of  $\gamma$  at these temperatures. The solid line in Fig. 9 represents an exponential fit to the experimental data and provides the following Arrhenius expression for  $\gamma$ :

$$\gamma = (2.3 \pm 0.9) \times 10^{-3} \exp[(-1910 \pm 130)/T]$$

at  $T = 275\text{--}320$  K (uncertainties are  $1\sigma$  statistical ones).

### 3.5 Dependence on O<sub>2</sub> concentration

In this series of experiments the uptake coefficient of NO<sub>2</sub> was measured in the presence of O<sub>2</sub> in the reactor. The partial pressure of oxygen was varied between 0.002 and 3 Torr, the total pressure (O<sub>2</sub> + He) in the reactor being near 10 Torr. The results of these experiments are shown in Fig. 10. A slight inverse dependence of the uptake coefficient on O<sub>2</sub> pressure is observed: an increase of the oxygen pressure by three orders of magnitude leads to a decrease of  $\gamma$  by a factor of 3. Similarity of the data observed with different RH (0.9 and 36 %) indicates that the uptake coefficient remains independent of the relative humidity in the whole range of oxygen concentrations used. The solid line in Fig. 10 represents a fit to the experimental data and corresponds to the following expression:

$$\gamma = 3 \times 10^{-6} / (1 + P^{0.36})$$

where  $P$  is the partial pressure of O<sub>2</sub> (in Torr).

## 4 Discussion

The results of the present study can be compared with available data from previous studies. The dark reaction of NO<sub>2</sub> with TiO<sub>2</sub> surface was investigated in three studies using a Knudsen cell reactor coupled to a quadrupole mass spectrometer (Underwood et al., 1999, 2001; Setyan et al., 2009). The following values were determined by Underwood et al. (1999, 2001) for the initial uptake coefficient ( $[\text{NO}_2]$  being varied from  $3 \times 10^{11}$  to  $3 \times 10^{14} \text{ molecule cm}^{-3}$ ):  $\gamma_0(\text{dark}) = 4 \times 10^{-4}$  using geometric surface area and  $\sim 10^{-7}$  for the uptake coefficient, corrected for the effect of bulk diffusion. The value of  $\gamma_0(\text{dark}) = 6 \times 10^{-6}$  determined in the present study using BET surface area, lies between the above two values. On the contrary, Setyan et al. (2009) have not observed any NO<sub>2</sub> uptake on the TiO<sub>2</sub> surface. Although these authors did not give any estimation of the upper limit of the uptake coefficient, simple calculations show that the value of  $\gamma_0$  from the present study would lead to an initial drop of NO<sub>2</sub> signal at least by a factor of 1.5 under their experimental conditions. The reason for the lower NO<sub>2</sub> uptake to TiO<sub>2</sub> surface in the study of Setyan et al. (2009) compared with the present one, could be the mode of preparation of solid samples. Note that in the present work TiO<sub>2</sub> samples were heated under pumping prior to uptake measurements.

A deactivating behaviour of TiO<sub>2</sub> in the reaction with NO<sub>2</sub> under UV irradiation observed in the present study supports the previous observations of Ohko et al. (2008). These authors have observed that the photocatalytic activity was decreased with accumulation of HNO<sub>3</sub> on the TiO<sub>2</sub> surface and concluded that the produced HNO<sub>3</sub> inhibited the photocatalytic heterogeneous reaction as a physical barrier. They reported that, when the steady state was reached, the photocatalytic activity remained at nearly 8% of the initial one. This value is in a fair agreement with a few percent steady state photocatalytic activity observed in the present study. In contrast to these two studies, time independent uptake of NO<sub>2</sub> on TiO<sub>2</sub> films was observed by Ndour et al. (2008): no surface deactivation has been observed on the synthetic TiO<sub>2</sub>/SiO<sub>2</sub> samples exposed over hours to NO<sub>2</sub> concentrations up to 300 ppb. In several previous studies (e.g. Lin et al., 2006; Ohko et al., 2008) it was observed that the photocatalytic activity of the TiO<sub>2</sub> film can be fully regenerated after rinsing with water. In the present work, we have observed similar behaviour: the deactivated TiO<sub>2</sub> sample was regenerated after being immersed in water.

Gustafsson et al. (2006) studied the uptake of NO<sub>2</sub> on illuminated P25 TiO<sub>2</sub> aerosols using initial NO<sub>2</sub> concentrations similar to those of the present study ( $\approx 2 \times 10^{12} \text{ molecule cm}^{-3}$ ). The measured uptake coefficient was found to negatively correlate with relative humidity and to range from  $9.6 \times 10^{-4}$  for 15% RH to  $1.2 \times 10^{-4}$  for 80% RH. Considering the method used by Gustafsson et al. (2006) (continuous flow of the aerosol/NO<sub>2</sub> mixture, i.e. rather short aerosol to NO<sub>2</sub> exposure times) these values should

be considered as corresponding to initial uptake and can be compared with  $\gamma_0 = 1.2 \times 10^{-4}$  determined in the present study under dry conditions. Agreement between the results from the two studies seems to be reasonable, especially if one considers that the uptake coefficients measured by Gustafsson et al. (2006) seem to represent an upper limit of  $\gamma_0$  because the aerosol surface area available for the reaction was calculated from the measured aerosol size distribution by assuming that the particles have the same surface areas as spheres of the same electrical mobility. Gustafsson et al. (2006) observed a negative correlation between the HONO formation rate in the reaction of  $\text{NO}_2$  with  $\text{TiO}_2$  and relative humidity. This behaviour was interpreted as a result of increased water adsorption inhibiting  $\text{NO}_2$  adsorption and/or electron/hole transfer processes at the  $\text{TiO}_2$ /gas interface. In the present study the impact of RH on the initial uptake of  $\text{NO}_2$  has not been studied, however we have not observed any influence of RH on the uptake coefficient of  $\text{NO}_2$  under steady state conditions.

The only value for the steady state uptake coefficient of  $\text{NO}_2$  on an irradiated pure  $\text{TiO}_2$  surface was reported by Monge et al. (2010). These authors measured  $\gamma = 1.5 \times 10^{-6}$  at  $T = 298 \text{ K}$ , 30 % relative humidity under atmospheric pressure of  $\text{N}_2$  and  $[\text{NO}_2] = 3.8 \times 10^{12} \text{ molecule cm}^{-3}$ . This value is in a good agreement with that measured in the present study at  $T = 298 \text{ K}$ :  $\gamma \approx 3.8 \times 10^{-6}$  (see Fig. 9). However, it should be noted that when comparing the above two numbers one should consider that the results were determined under different irradiance conditions, the  $\text{NO}_2$  photolysis rate being  $6 \times 10^{-3}$  and  $4.75 \times 10^{-4} \text{ s}^{-1}$  in the present study and in Monge et al. (2010), respectively.

It is also interesting to compare the data on  $\text{NO}_2$  uptake to pure  $\text{TiO}_2$  from the present study with those measured on mineral dust originating from different locations of the Sahara desert (Ndour et al., 2009b). The reported uptake coefficients of  $\text{NO}_2$  (25 ppb) on four different Sahara sand samples were between 0.35 and  $1.46 \times 10^{-7}$  at  $T = 298 \text{ K}$ , 25% relative humidity, in an atmosphere of  $\text{N}_2$ . The value of  $\gamma$  measured in the present study on pure  $\text{TiO}_2$  under these conditions is near  $8 \times 10^{-6}$  (from Fig. 6 and temperature dependence of  $\gamma$ ), i.e. by a factor of 50–200 higher. Considering that  $\text{TiO}_2$  content in the sand samples used by Ndour et al. (2009b) was between 0.2 and 1 wt% and assuming that their photoreactivity was mainly due to  $\text{TiO}_2$ , the agreement between the results observed on pure  $\text{TiO}_2$  (present study) and real dust samples with low  $\text{TiO}_2$  content (Ndour et al., 2009b) seems to be very satisfactory.

So far, the effect of oxygen on the rate of  $\text{NO}_2$  loss on irradiated  $\text{TiO}_2$  surface has been considered only in one study (Monge et al., 2010). These authors have observed that the uptake coefficient of  $\text{NO}_2$  on pure  $\text{TiO}_2$  was highly influenced by the presence of  $\text{O}_2$ , and reported a value of  $\gamma$  one order of magnitude higher in 1 atm of  $\text{N}_2$  compared with that in  $\text{N}_2\text{:O}_2$  (85 %:15%) mixture. Interestingly, the application of the expression for the dependence of  $\gamma$  on the pressure

of  $\text{O}_2$  from the present study,  $\gamma \sim (1 + P^{0.36})^{-1}$ , to the experimental conditions used by Monge et al. (2010), gives a factor of 6.5 for the expected difference between the values of  $\gamma$  in presence and absence of oxygen. This seems to indicate that the analytic expression for the dependence of  $\gamma$  on  $\text{O}_2$  pressure derived in the present study at rather low pressures of oxygen is applicable under atmospheric conditions. The effect of oxygen was suggested to be due to competition between  $\text{O}_2$  and  $\text{NO}_2$  for scavenging the electrons at the surface of the photocatalyst (Monge et al., 2010).

The extended data set obtained in the present study for the uptake coefficient of  $\text{NO}_2$  to the  $\text{TiO}_2$  surface seems to allow calculating  $\gamma$  values for atmospheric conditions. Dependencies of  $\gamma$  on temperature and pressure of oxygen can be combined, giving the following final expression for  $\gamma$ :

$$\gamma = \frac{2.3 \times 10^{-3} \exp(-1910/T)}{1 + P^{0.36}}$$

where  $T$  is the temperature (K) and  $P$  is the oxygen pressure (Torr). This expression is applicable for any atmospheric relative humidity and for  $J_{\text{NO}_2} = 0.006 \text{ s}^{-1}$ . Let's note that the dependence on the photon flux is not significant, at least, in the range of  $J_{\text{NO}_2}$  values between 0.002 and  $0.012 \text{ s}^{-1}$  considered in the present study. An important parameter in the calculation of  $\gamma$  is the concentration of  $\text{NO}_2$ . The above expression was derived from the experiments carried out with  $[\text{NO}_2] \approx 2 \times 10^{12} \text{ molecule cm}^{-3}$  (nearly 90 ppb for  $P = 1 \text{ atm}$ ). As shown in Fig. 6, at lower  $\text{NO}_2$  concentrations the value of  $\gamma$  will be higher.

The atmospheric and environmental impact of the interaction of  $\text{NO}_2$  with irradiated  $\text{TiO}_2$ -containing mineral aerosols and depolluting materials is strongly dependent on the gaseous and surface bound products of this process. In previous studies, HONO (Gustafsson et al., 2006; Ndour et al., 2008; Monge et al., 2010; Beaumont et al., 2009) and NO (Ohko et al., 2008; Monge et al., 2010) in the gas phase as well as nitric acid/nitrate anion on the surface (e.g. Dalton et al., 2002; Devahasdin et al., 2003; Lin et al., 2006; Ndour et al., 2008; Negishi et al., 1998; Ohko et al., 2008) were observed as the  $\text{NO}_2 + \text{TiO}_2$  reaction products. In the present study we have observed HONO, NO and, in addition,  $\text{N}_2\text{O}$  to be released into the gas phase as a result of the heterogeneous reaction of  $\text{NO}_2$  with  $\text{TiO}_2$  surface. The formation of  $\text{NO}_3^-$  on the surface of the  $\text{TiO}_2$  sample was also observed by means of ion chromatography. The individual yields of the gas phase products were found to be strongly dependent on the experimental conditions such as relative humidity, temperature and concentration of oxygen in the reactive system. A detailed product study of the heterogeneous  $\text{NO}_2 + \text{TiO}_2$  reaction is a subject of our current work and will be published in a separate paper.



**Acknowledgements.** This study was supported by LEFE – CHAT programme of CNRS (Photona project) and the ANR Photodust project. A. E. Z. is very grateful to région Centre for financing his PhD grant.

Edited by: M. Ammann



The publication of this article is financed by CNRS-INSU.

## References

- Beaumont, S. K., Gustafsson, R. J., and Lambert, R. M.: Heterogeneous Photochemistry Relevant to the Troposphere:  $\text{H}_2\text{O}_2$  Production during the Photochemical Reduction of  $\text{NO}_2$  to HONO on UV-Illuminated  $\text{TiO}_2$  Surfaces, *Chem. Phys. Chem.*, 10, 331–333, 2009.
- Bedjanian, Y., Lelièvre, S., and Le Bras, G.: Experimental study of the interaction of  $\text{HO}_2$  radicals with soot surface, *Phys. Chem. Chem. Phys.*, 7, 334–341, 2005.
- Dalton, J. S., Janes, P. A., Jones, N. G., Nicholson, J. A., Hallam, K. R., and Allen, G. C.: Photocatalytic oxidation of  $\text{NO}_x$  gases using  $\text{TiO}_2$ : a surface spectroscopic approach, *Environ. Pollut.*, 120, 415–422, 2002.
- Devahasdin, S., Fan Jr, C., Li, K., and Chen, D. H.:  $\text{TiO}_2$  photocatalytic oxidation of nitric oxide: transient behavior and reaction kinetics, *J. Photoch. Photobio. A*, 156, 161–170, 2003.
- Gustafsson, R. J., Orlov, A., Griffiths, P. T., Cox, R. A., and Lambert, R. M.: Reduction of  $\text{NO}_2$  to nitrous acid on illuminated titanium dioxide aerosol surfaces: implications for photocatalysis and atmospheric chemistry, *Chem. Commun.*, 3936–3938, 2006.
- Henderson, M. A.: A surface science perspective on photocatalysis, *Surf. Sci. Rep.*, 66, 185–297, 2011.
- Ibusuki, T. and Takeuchi, K.: Removal of low concentration nitrogen oxides through photoassisted heterogeneous catalysis, *J. Mol. Catal.*, 88, 93–102, 1994.
- Karagulian, F., Santschi, C., and Rossi, M. J.: The heterogeneous chemical kinetics of  $\text{N}_2\text{O}_5$  on  $\text{CaCO}_3$  and other atmospheric mineral dust surrogates, *Atmos. Chem. Phys.*, 6, 1373–1388, doi:10.5194/acp-6-1373-2006, 2006.
- Langridge, J. M., Gustafsson, R. J., Griffiths, P. T., Cox, R. A., Lambert, R. M., and Jones, R. L.: Solar driven nitrous acid formation on building material surfaces containing titanium dioxide: A concern for air quality in urban areas?, *Atmos. Environ.*, 43, 5128–5131, 2009.
- Laufs, S., Burgeth, G., Duttlinger, W., Kurtenbach, R., Maban, M., Thomas, C., Wiesen, P., and Kleffmann, J.: Conversion of nitrogen oxides on commercial photocatalytic dispersion paints, *Atmos. Environ.*, 44, 2341–2349, 2010.
- Lin, Y.-M., Tseng, Y.-H., Huang, J.-H., Chao, C. C., Chen, C.-C., and Wang, I.: Photocatalytic Activity for Degradation of Nitrogen Oxides over Visible Light Responsive Titania-Based Photocatalysts, *Environ. Sci. Technol.*, 40, 1616–1621, 2006.
- Monge, M. E., D'Anna, B., and George, C.: Nitrogen dioxide removal and nitrous acid formation on titanium oxide surfaces-an air quality remediation process?, *Phys. Chem. Chem. Phys.*, 12, 8991–8998, 2010.
- Ndour, M., D'Anna, B., George, C., Ka, O., Balkanski, Y., Kleffmann, J., Stemmler, K., and Ammann, M.: Photoenhanced uptake of  $\text{NO}_2$  on mineral dust: Laboratory experiments and model simulations, *Geophys. Res. Lett.*, 35, L05812, doi:10.1029/2007GL032006, 2008.
- Ndour, M., Conchon, P., D'Anna, B., Ka, O., and George, C.: Photochemistry of mineral dust surface as a potential atmospheric renoxification process, *Geophys. Res. Lett.*, 36, L05816, doi:10.1029/2008GL036662, 2009a.
- Ndour, M., Nicolas, M., D'Anna, B., Ka, O., and George, C.: Photoreactivity of  $\text{NO}_2$  on mineral dusts originating from different locations of the Sahara desert, *Phys. Chem. Chem. Phys.*, 11, 1312–1319, 2009b.
- Negishi, N., Takeuchi, K., and Ibusuki, T.: Surface structure of the  $\text{TiO}_2$  thin film photocatalyst, *J. Mater. Sci.*, 33, 5789–5794, 1998.
- Ohko, Y., Nakamura, Y., Fukuda, A., Matsuzawa, S., and Takeuchi, K.: Photocatalytic Oxidation of Nitrogen Dioxide with  $\text{TiO}_2$  Thin Films under Continuous UV-Light Illumination, *J. Phys. Chem. C*, 112, 10502–10508, 2008.
- Setyan, A., Sauvain, J. J., and Rossi, M. J.: The use of heterogeneous chemistry for the characterization of functional groups at the gas/particle interface of soot and  $\text{TiO}_2$  nanoparticles, *Phys. Chem. Chem. Phys.*, 11, 6205–6217, 2009.
- Underwood, G. M., Miller, T. M., and Grassian, V. H.: Transmission FT-IR and Knudsen Cell Study of the Heterogeneous Reactivity of Gaseous Nitrogen Dioxide on Mineral Oxide Particles, *J. Phys. Chem. A*, 103, 6184–6190, 1999.
- Underwood, G. M., Song, C. H., Phadnis, M., Carmichael, G. R., and Grassian, V. H.: Heterogeneous reactions of  $\text{NO}_2$  and  $\text{HNO}_3$  on oxides and mineral dust: A combined laboratory and modeling study, *J. Geophys. Res.*, 106, 18055–18066, 2001.